UNIVERSITY OF ARKANSAS

Graduate Institute of Technology

A FEASIBILITY STUDY ON DETERMINATION OF THE DEVIATION FROM LEVEL UTILIZING OPTICAL INTERFERENCE CREATED BY A LASER SOURCE

George H. Cline

Master of Science Thesis
Department of Electronics and Instrumentation
1971

A FEASIBILITY STUDY ON DETERMINATION OF THE DEVIATION FROM LEVEL UTILIZING OPTICAL INTERFERENCE CREATED BY A LASER SOURCE

A FEASIBILITY STUDY ON DETERMINATION OF THE DEVIATION FROM LEVEL UTILIZING OPTICAL INTERFERENCE CREATED BY A LASER SOURCE

A thesis submitted in partial fulfillment
of the requirements for degree of
Master of Science

By

George H. Cline, B.S.
Kansas State College of Pittsburg, 1964

1971
The University of Arkansas

This Thesis is approved
for recommendation to the
Graduate Council

Major Professor:

Thesis Committee:

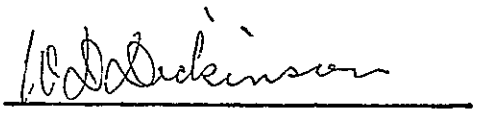

_____

ACKNOWLEDGMENTS

The author wishes to express his appreciation for the freedom of self direction allowed by his major professor Dr. M. K. Testerman; the helpful answers to electronic questions given by Professor R. W. Raible; and the helpful debates with Professors P. C. McLeod and W. D. Dickinson. Particular acknowledgment must be given to peer J. McElroy whose skepticism encouraged thoroughness.

This research was supported in part by NASA Grant NGL 04-001-007 (Formerly NsG 713).

TABLE OF CONTENTS

LIST OF TABLES

LIST OF FIGURES

Figure

INTRODUCTION

The level referred to herein is a geoid or plane perpendicular to the force of gravity at any point in an existing gravitational field. This study was undertaken to establish the feasibility of using the interference effects within an optical wedge, one side of which is a liquid surface, to determine the exactness to which this geoid can be approached. It is a new application of established physical laws toward effecting an absolute measurement.

When properly illuminated, an optical wedge spawns visible interference phenomena. Such a wedge is formed by an optical flat suspended a small distance above a liquid surface and canted slightly so that the planes containing the liquid and flat surfaces are not parallel. Since a small area of a liquid surface forms the partial surface of a geoid, the interference phenomena resulting from the wedge will be indicative of the wedge angle existing between the surface of the flat and the geoid. These interference phenomena will also indicate the direction of the wedge angle.

The characteristics of these interference phenomena are determined by the characteristics of the source of illumination, by the surfaces forming the optical wedge,

by the wedge composition (glass, water, air, etc.) and by the angle magnitude and direction. This study investigates the characteristics of the interference phenomena resulting from specific materials used as the source, surfaces and wedge composition in an effort to test the feasibility of using these characteristics to establish an object's degree of deviation from level. The purpose is to determine if a more practical, sensitive, accurate and readily automated leveling device, ~~than presently exists~~, can be developed.

LITERATURE SURVEY

Existing Levels

Most devices used today to determine the degree of level are spirit or bubble levels. They are not necessarily used to determine the degree of level but are used to set a device (telescope, theodolite, alidade or other object) as level as possible. They consist of a tube or spherical topped container filled with a liquid except for an air space or bubble which rises to the top of the container, the top being that opposite the force of gravity. Thus, with proper calibration, this device can be used to determine the level or degree of level.

The greatest causes of inaccuracies are dissimilar thermal expansion of components and adhesion of liquid to container. The first causes the bubble to change size, thus calibration is lost; the second causes the bubble not to move as the container is tilted. The accuracy is proportional to the radius of the top of the container; the limit or maximum determinable angle is inversely proportional to the radius. Thus, compromises are made to meet specific requirements.

Another device is the auto-collimator type level. This level relies on reflections of images from two

surfaces and the alignment or superposition of these images. One surface (for instance, a liquid or a pendulous mirror or optical flat) is initially level and naturally maintains its position. The other surface is then adjusted or leveled by superimposition of the reflected images. The images can be projected slits, apertures, crosshairs, and so on. This device has greater inherent accuracy but not necessarily greater sensitivity than the bubble device. However, its sensitivity and ultimate accuracy are governed by the laws of reflection and refraction which are rather severe limitations when compared with the limiting factors of the device proposed herein.

Both general types of levels described above have many refinements to alleviate or eliminate the difficulties mentioned. A further discussion may be found in a book by Martin[9].

Both types rely on the human eye for determinations. They would be difficult, if not impossible, to automate. Determination of the level to less than one second with devices of reasonable dimensions would be stretching the imagination. These factors led to the feasibility study undertaken herein.

Proposal

The object of this study is to test the feasibility of a proposal of using an optical wedge in the determination of the degree of level. One surface of the wedge will be a suitable liquid, the other a circular optical flat. (This wedge is illustrated in Figure 1.) The interference phenomena formed within a perfect optical wedge (i.e., the two surfaces considered to be geometric planes) when illuminated with collimated light are equally spaced parallel fringes. However, the surface of the liquid forms a partial sphere, the radius of which equals that of the earth. This causes the ends of the parallel fringes to bend in toward the middle as they follow contours of equidistant separation. Likewise, the glass flat causes a similar effect because it sags. A theoretical and experimental discussion of this is found in an article by Emerson[6]. It will be apparent, as the discussion progresses, that both of these effects can be neglected. Because of the method of readout, the lack of parallelism of the fringes does not affect accuracy or sensitivity.

The intersection of the planes of the two wedge surfaces runs parallel to the fringes, thus the direction of the wedge angle can be easily determined. As

the wedge angle decreases, the distance between the parallel fringes increases, thus there are fewer fringes per given area; as the angle increases, the distance decreases, thus there are more fringes per given area. As the apex of the wedge angle changes direction, the fringes change orientation so as to indicate the direction of the apex as noted above. A mathematical treatment of the interference phenomena follows.

These parallel fringes follow contours of equidistant separation as noted above. Illumination of any spot on a particular contour spawns similar interference phenomena. A fringe existing within this spot would extend across the wedge if the wedge were wholly illuminated. If the spot is sufficiently small with respect to the fringe width, the intensity of the interference phenomena within the spot varies similarly to that of Figure 2 as the spot crosses the fringes. Thus, scanning the sufficiently small spot about the periphery of the flat yields the same information as illumination of the whole flat would yield.

The spot of illumination amounts to a shaft of visible radiation, in this proposal, a laser. Most treatments in the literature, for example, Oppenheim[10],

use broad sources, thus the fringes are localized near the wedge surfaces and are visible in widely varying directions. The fringes formed by the laser or shaft of collimated radiation are visible only within the reflected shaft as when intercepted by a detector, usually the eye. A broad source creates scattering at the wedge, allowing the fringes to be visible from various directions, but there is little scattering of a laser beam as it strikes a clean, smooth glass surface. The use of a laser beam instead of a broad source makes possible a treatment that is somewhat more simple. The interference phenomena are not localized at or about the optical wedge, but are what this author would call "standing" the full length of the shaft of reflected light. In other words, the whole length of the reflected beam exhibits interference phenomena that exist at the point of illumination in the wedge. Regardless of the point of interception of the beam, the detector registers the same interference phenomena, if all else is maintained unchanged.

The term "reflected light" used above is an important descriptive term, for it is the reflected beams and concomitant interference phenomena that this proposal

uses. The reflection from the lower or flat surface of the optical flat interferes with the reflection from the surface of the liquid. Refer to Figure 1 for illustration. In this Figure, R_f and R_l represent the intensities of the reflected beams. The wedge angle 0 is highly exaggerated to show detail. I_t, the transmitted beam intensity has little if any detectable interference phenomena imposed upon it. Multiple-beam interferometry is needed to create visible interference phenomena by transmission, which in turn requires the wedge surfaces to be highly reflective. Since the liquid and flat surfaces have reflectivities of about 4 percent, only the reflected beams exhibit highly visible interference. It is desired to have R_f as nearly equal to R_l as possible, so that when the two beams are 180 degrees out of phase equivalent to any integral of 1/2 wavelength surface separation, complete destructive interference occurs resulting in zero light intensity, as indicated in Figure 2.

The interference phenomena registered by the detector can be derived using the Doppler effect. The reflection from the liquid surface, the frequency of which does not vary with time, can be considered the local oscillator. The reflection from the flat

varies in frequency as the point of illumination on the flat surface recedes and proceeds as the flat is scanned These two reflections are heterodyned on the detector surface yielding the resultant signal. However, since the apparent velocity of the flat surface is considerably less than that in the criteria derived by Burgess[4] to make a Doppler treatment mandatory, this author will use a regular interference treatment.

Since the reflectivities of the flat and liquid surfaces are so low (4 percent), for a good approximation the interference phenomena can be considered to be created by two beam division of amplitude type interference[1]. From Figure 1, R_f and R_l are the intensities of the two beams, then from Born and Wolf[2], with only a change in nomenclature, the resultant intensity I from the interference of R_f and R_l is

$$I = R_f + R_l + 2\sqrt{R_f R_l} \cos \delta \qquad (1)$$

where δ is the phase angle between the electric vectors of the two beams. Equation 1 is obviously a maximum when δ equals even multiples of π and is a minimum when δ equals odd multiples of π. When R_f equals R_l, Equation 1 reduces to

$$I = 4R_f \cos^2(\delta/2). \qquad (2)$$

Equation 2 is used to describe the intensity variation of the reflected beams as shown in Figure 2. It will be insured that R_f does not vary greatly from R_1; thus, Equation 2 is approximately equal to Equation 1. The use of Equation 2 is desired so that later sensitivity calculation will be simplified. In Equation 2, the argument of the cosine obviously equals $(\frac{2\pi n2h}{\lambda_0} + \pi)$ where n is the index of refraction of the material within the wedge (in this case air - $n \simeq 1$), λ_0 is the vacuum wavelength of the incident radiation, h is the surface separation and π accounts for the 180 degree phase shift upon reflection from the air-liquid interface. Thus,

$$\cos^2(\delta/2) = \cos^2(\frac{2\pi n2h}{2\lambda_0} + \pi/2) = \sin^2(\frac{2\pi nh}{\lambda_0}).$$

Therefore, Equation 2 evolves to

$$I = 4R_f \sin^2(2\pi h/\lambda_0) \qquad (3)$$

where the value of n equal to 1 has been used. Equation 3 in conjunction with Figure 3 shows that for I to be a maximum, h equals $\frac{k\lambda}{4}$, $\frac{(k+2)\lambda}{4}$, $\frac{(k+4)\lambda}{4}$, . . ., where k refers to the order of the interference and in this case can equal any one of the possible numbers (1, 3, 5, 7, ...). In Figure 3, L is the fringe separation and θ is the wedge angle or "level angle". To

reiterate, it is this angle, the angular amount that the flat is off level, that can be determined by the fringe count over a given area of the flat.

Consideration is now given to the method of scanning the beam about the periphery of the flat. The method used in this study is that illustrated in Figures 4 and 10 (refer to tabulated components of the Figures in Table 1) where all mirrors are of the front surfaced totally reflecting type. The laser beam is reflected downward perpendicular to the liquid surface by mirror M_1. It is reflected horizontally by M_2 and again downward perpendicular to the liquid surface by M_3. M_2 and M_3 are stationary with respect to each other and both rotate together about the center line formed by the beam between mirrors M_1 and M_2. Upon reflection from the flat and liquid surfaces the two resulting beams nearly retrace this path, but are reflected at a slight angle and bypass M_1 and strike a detector mounted above M_1. The cause and means of accomplishing this will be discussed later.

The reflections from the front surface mirrors create another interesting phenomenon, that of elliptically polarized light. The net result will not affect the results of this study to any detectable extent.

A brief explanation will follow to verify the fact that the interference phenomena that are used in this study are not affected by elliptically polarized light.

Elliptically polarized light is considered composed of two components polarized perpendicular to each other. In most treatments of polarization by reflection, for example, Ditchburn[5], the components are designated as perpendicular or parallel to the plane of incidence. Likewise, here $A_{\perp}$ indicates the perpendicular component and $A_{\parallel}$ indicates the parallel component. The reflection coefficient and the phasal relationship of the two reflected components varies as the angle of incidence. Since the angle of incidence is 45 degrees for all the mirrors used in this study, these two qualities remain constant.

Referring to Figure 4, as M_2 and M_3 rotate, $A_{\perp}$ and $A_{\parallel}$ vary sinusoidily at the rate of rotation. Each go through zero to a maximum and back. For instance, when M_2 and M_3 are positioned as shown and the electric vector of the laser beam is in the plane of the paper, $A_{\parallel}$ is maximum and $A_{\perp}$ is zero. With $\pi/2$ radians of rotation of M_2 and M_3, the opposite is true. According to Born and Wolf[3], the phasal difference of the two components upon reflection at 45 degrees for a typical metal is

about π radians per reflection. There are four reflections of concern; the initial reflections from M_2 and M_3 and the reflections from M_2 and M_3 of the beam as the incident path is retraced by the reflections from the surfaces of the flat and liquid. The reflection from M_1 is inconsequential because adjustment of the laser can be made to cause all the incident radiation to be either $A_\perp$ or $A_\parallel$ with respect to M_1. Again, from Born and Wolf[3], the phase angle between components after four reflections from a typical metal is about $\pi/2$ radians. This would yield circularly polarized light if $A_\perp$ equaled $A_\parallel$. But $A_\perp$ equals $A_\parallel$ only four times every rotation of M_2 and M_3 and the phase angle is only approximately equal to $\pi/2$ radians. Thus, elliptically polarized light results with the eccentricity of the ellipse varying between zero and one along with the axis of the ellipse rotating.

Components of light polarized at 90 degrees with respect to each other, as with elliptically polarized light, cannot interfere with each other. Thus, any interference that occurs must result from the interference within each component. This is indeed what happens. Each component can be considered a separate laser beam and all the descriptive equations derived earlier remain valid.

The detector used is a silicon diode. It has an efficiency of about 12 percent. A discussion of operation and characteristics of a silicon diode is found in Van Der Ziel[14].

A laser is used in this study for several reasons. It is a highly monochromatic, collimated and intense beam. These three characteristics are desirable in this study. There is no practical way of creating a beam, from conventional sodium or mercury sources, having the characteristics of a laser beam. The filtering for as narrow a spectral width would be impossible. The losses in the filtering, focusing and collimating optics would make intensity simulation a task impossibly difficult.

Coherence length is commonly defined by the equation

$$\Delta l = c/\Delta\nu \qquad (4)$$

where Δl is coherence length, c is speed of light and $\Delta\nu$ is band width or line width. Because of the high monochromaticity of a laser beam, $\Delta\nu$ is extremely small and Δl is in terms of meters rather than millimeters or centimeters as with conventional sources. Interference phenomena cannot occur if the difference in path length between the two interfering beams exceeds the coherence length. Also, the fringe visibility varies inversely

with the fraction (difference in path length)/(coherence length) when the fraction is less than 1, otherwise the visibility is zero. This means that with a laser source separation of the liquid and flat surfaces can be theoretically of the order of meters with little or no loss in visibility. In addition, this allows the system to be more rugged, the greater possible surface separation means that the liquid is less likely to contact and wet the flat surface, thus making the system inoperative. Also, the intensity of the laser used is sufficient to allow the use of a silicon diode for detection, obviating the need of a photomultiplier and associated power supply.

To increase the limits on the maximum detectable angle, it is proposed that a lens be used. It will be placed in the laser beam and have a focal length such that the beam will be focused to a point between the liquid and flat surfaces. Since the size of the point of focus is smaller than the original beam, fringes closer together can be resolved. Thus, a greater off-level angle can be resolved and determined. The inclusion of this lens presents another problem, point sources separated in depth and their concomitant interference phenomena, which will be discussed later.

Mathematical Treatments

The following discussion involves theory, the recognition of affecting variables and other considerations that must be made. The author thinks that this discussion can best be accomplished by mathematical treatments, some of which are rigorous, some not so rigorous. The result will be an introduction to all the considerations that must be made along with the mathematics that will give some indication of the means of treating these considerations. All necessary dimensions used will be taken from the experimental setup. Since some of the dimensions are only approximate, the results of calculations are only approximate also, but the idea is to present theory and obtain usable answers in one operation.

(a) The Wedge

The object is to determine the magnitude of the off-level angle, θ, in Figure 3 via the fringe separation L. The distance, L, will be determined by dividing the scan diameter by one-half the number of fringes within the scan since the fringes are counted twice for each complete revolution. Figures 3 and 4 will be used for reference and explanation. For all values of θ, (all of which will be less than 5 degrees as shall be

proven presently) a linear relationship can be assumed to exist between θ and L.

From Figure 3 it is seen that the vertical differential of the flat between fringes is $\lambda/2$. Therefore, θ equals $(\lambda/2)/L$ radians where λ is wavelength of source of illumination (6328 angstroms). As L approaches infinity, θ approaches zero. In other words, if there are no fringes across the flat, θ equals 0 and the flat is absolutely level. When L is less than infinity, θ equals $6.52/L$ sec where L is in centimeters or θ equals $6.52N/2D$ where N equals the number of fringes per scan revolution; D is the scan diameter and equals 9.8 centimeters from the experimental setup. A plot of this equation will provide quick interpretation of the off-level angle when the number of fringes are known. Two points are needed for the plot. One is easily obtained; when N equals zero, θ equals zero. The other can be obtained by assuming a number of fringes, for instance 80; θ equals 26.6 sec. This plot, shown in Figure 5, will be used to interpret experimental data.

(b) Maximum Sensitivity and Accuracy

With less than one fringe, the angle θ must be determined by measuring the variation in change in intensity across the flat. The relationship between

angle and intensity is not linear as is evident in Figure 2. It is apparent that maximum sensitivity occurs at separation of odd integrals of $\lambda/8$. That is, maximum change of intensity occurs for a given change in surface separation (refer again to Figure 2). Therefore, to determine the absolute level with the greatest accuracy, the surface separation must approach an odd integral of $\lambda/8$ over the entire area of the flat as the condition of level is approached.

To determine the change in intensity with change in surface separation, Equation 3 is differentiated with respect to h. Thus,

$$\frac{dI}{dh} = \frac{16\pi R_f}{\lambda_0} \sin\left(\frac{2\pi h}{\lambda_0}\right) \cos\left(\frac{2\pi h}{\lambda_0}\right). \tag{5}$$

Rearranging and dividing by Equation 3,

$$\frac{\Delta I}{I} = \frac{4\pi}{\lambda_0} \frac{\cos(2\pi h/\lambda_0)}{\sin(2\pi h/\lambda_0)} \Delta h, \tag{6}$$

and, since $\sin(2\pi h/\lambda_0)$ equals $\cos(2\pi h/\lambda_0)$, when h equals odd integrals of $\lambda_0/8$

$$\frac{\Delta I}{I_0} = \frac{4\pi}{\lambda_0} \Delta h \tag{7}$$

where I_0 equals 1/2 maximum intensity. Assume a 10 percent variation in intensity to be discernible. Then Δh

would be 5.04×10^{-7} centimeters. Assuming this variation was detected as the flat was scanned, this would give θ equal to 1.06×10^{-2} sec. In this "best" case analysis, the 1.06×10^{-2} sec is both the accuracy and sensitivity. Of course only at wedge surface separations of odd integrals of $\lambda/8$ can this accuracy and sensitivity be realized. These separations can be effected by varying the index of refraction of the medium (air) within the wedge, i.e., by evacuating it, or by piezo-electrically displacing the liquid, thus raising or lowering the surface.

As the condition of level is approached and there is no discernible signal resulting from a scan around the flat, the optical path length is varied by $\lambda/2$ by a method suggested above. From Figure 2 it is seen that this will provide calibration and a ready determination of (1/2)I maximum (the operation point). Of course, continual check will be needed to correct for changes caused by temperature variations and other effects. The later method suggested above was to be tried in this study. Difficulties arose, as discussed in the Discussion of Results section, which prevented this accuracy and sensitivity determination.

(c) Two Sources Separated in Depth

The converging beam, upon striking the flat and liquid surface, will begin diverging as it passes the focal point of the lens. The diverging reflections will form two point sources, one real and one imaginary, separated in depth as shown in Figure 6. The point sources will radiate within the same solid angle as the solid angle of incidence. Two point sources, both temporally and spatially coherent, separated in depth will yield interference fringes much like Newton's rings on a viewing surface. The two sources formed by the reflections meet these coherence requirements, thus the detector aperture must be limited to exclude the first circular fringe formed as a result of a $\lambda/2$ differential from the central fringe. If not limited, the circular fringes on the detector surface will expand or collapse as the flat and liquid surface separation is varied. This will yield an integrated signal resultant of zero. Equations for calculation of the radius of the first fringe can easily be obtained from Figure 7. Thus, two equations with two unknowns are:

$$x^2 + a^2 \simeq (a + k + \lambda/2)^2 \qquad (8)$$

$$x^2 + (a+b)^2 \simeq (a+b+k)^2 \qquad (9)$$

where a equals the distance from the nearest source to the detector (approximately 38 cm), b equals the distance between, or depth of, the sources (approximately 3 cm), x equals the radius of the first fringe of the $\lambda/2$ differential and k is a slack variable. Solving and neglecting second order terms yields x approximately equal to 1.8 mm. Since the diverging beam diameter is approximately equal to 1.3 mm at the detector and the radius of the first out of phase fringe is approximately equal to 1.8 mm, neither the first nor succeeding fringes are formed, thus it is not necessary to limit the detector aperture.

(d) Maximum Detectable Angle

Since the signal will not be affected by the interference phenomena resulting from sources separated in depth, it is apparent that the maximum detectable off-level angle will be determined by other considerations. One is the amount of beam overlap upon the detector surface necessary to provide a signal. This in turn depends upon the detector characteristics and the electronic circuitry. If the detector sees a high impedence load, there will be little electrical "loading". Theoretically if the load were of infinite impedence, beam overlap to provide energy of the order of a photon for

each beam within the overlap areas would be sufficient, that is, if the efficiency of the detector approached unity. More realistic appraisal would hint at allowing at least 1/2 beam diameter as minimum overlap. Then, from Figure 8, the maximum value of θ is approximately equal to $(a/2)/2d$ equals 212 sec where θ equals maximum detectable off-level angle. For the fringes representing this angle to be resolved, the maximum beam diameter at the flat and liquid surfaces should not exceed one-half the separation of the fringes. By simple triangulation and the use of geometrical optics and of Figure 6, the beam diameter at either surface, if the focal point of lens is centered between the two, is approximately 4.0×10^{-3} cm.

However, the minimum spot size or diameter to which a laser can be focused is ϕf where ϕ is the beam divergence and f is the focal length of the lens. The value of ϕ can be determined by

$$\phi = 1.22\lambda/a \qquad (10)$$

where λ is the wavelength of the radiation and a is the beam diameter. For the laser used, ϕ is less than 7×10^{-4} radians. Thus, D, the minimum spot diameter, can be said to be less than 0.027 cm in diameter. This

also means that the diameter of the beam at the surface of the liquid must be greater than 0.027 cm.

The fringe separation must therefore be at least 0.054 cm for the fringes to be resolved. This separation corresponds to an angle θ of 240 sec, the maximum detectable angle. Thus, the fringes that represent an angle of 212 seconds derived from beam overlap considerations can be resolved and 212 seconds stands as the maximum detectable off-level, because an angle of 240 seconds would cause less than one-half beam diameter overlap.

However, later calculations will change this result. A device is incorporated (a wedge) which causes a lateral displacement of R_f from R_l as illustrated in Figure 9. This lateral displacement is about 0.037 cm, a figure derived later. It is always in one direction, so that in this direction the maximum detectable angle is limited further. Referring to Figure 8, if R_l is displaced from R_f at the flat surface as illustrated in Figure 9, θ must be less in order to maintain one-half beam diameter overlap of R_l and R_f. Of course, this is in one direction. The maximum detectable angle due to overlap considerations will increase and exceed the 240 seconds as the direction of the off-level changes by 180 degrees.

A limit is now calculated which is valid in any direction. From an earlier equation, θ is approximately equal to $(a/2)/2d$. The numerator now must be replaced by $(a/2)-0.037$, which equals 0.028 cm, the linear distance at the detector that, in addition to the initial displacement of 0.037 cm, will provide one-half beam diameter overlap. Thus, θ is approximately equal to 74 seconds, the maximum detectable off-level angle.

(e) The Reflection From the Upper Surface of the Flat

The problem to be treated here resulted from experimental difficulties. It was originally assumed that an anti-reflective coating on the upper surface of the flat would eliminate this reflection, thus eliminating the interference phenomena associated with the reflections from the upper and lower flat surface. Early experimental data proved this not to be the case and led to the following calculations.

Magnesium fluoride was used as an anti-reflective coating. This material lowered the reflectivity of the upper surface of the flat to about 1 percent. With the 4 percent reflectivity from the liquid and lower surface, the ratio of the three is 1:4:4. With the aid of

Equation 1, it can readily be shown that the variation in amplitude of intensity resulting from the interference of the reflections from the upper and lower flat surfaces is 50 percent of that of the lower flat and liquid surfaces. This would make the ultimate sensitivity and accuracy previously calculated unobtainable and any signal difficult to interpret. Further lowering the reflectivity of the upper flat surface would be highly desirable. One manufacturer[8] stated that 0.1 percent reflectivity was probably impossible to obtain or measure and it would furnish a 0.5 percent anti-reflective coating. With this reflectivity, the ratio of variation in intensity of the two signals is 35 percent. These figures led to revised thinking and a new technique.

A wedge is used to replace the nearly parallel surface flat. The lower surface of the wedge and the liquid are still used to provide the desired reflectances, R_f and R_l. The reflectance from the upper surface is directed to the side as shown in Figure 9. R_f and R_l are also directed to the side by refraction and reflection. They are also displaced with respect to each other.

The location of the detector will now be determined. It is obviously not in line with the incident beam but to the side to intercept the reflected beams. Referring to Figure 9, ϕ_1 is 0.025 radians. Assuming the wedge to have an index of refraction of 1.5, it can be shown that ϕ_2 equals ϕ_1 (refer to Appendix A). The linear distance corresponding to ϕ_2 of the incident beam from the reflected beams R_f and R_1 in the plane of the detector is $\phi_2 d$ where d is the distance from the wedge to the detector. Thus, $\phi_2 d$ equals 0.95 cm. The lateral displacement of R_f and R_1 from I_i is negligible. Thus, the 0.95 cm displacement allows R_f and R_1 to bypass M_1 of Figure 4 as previously mentioned. The reflection from the upper surface of the wedge need not be considered further, for it is reflected in the opposite direction. The detector can be positioned to be missed easily by it.

The displacement of R_f and R_1 with respect to each other will affect the maximum detectable angle as previously calculated. By simple trigonometric relationships, it can be shown that the displacement is less than $\phi_1 h$ (refer to Appendix A) where ϕ_1 and h are identified in Figure 9. The quantity $\phi_1 h$ equals 0.037 cm. This value was used in previous calculations.

EXPERIMENTAL PROCEDURE

Equipment

Vibrations were a problem in this study, as they are with nearly all interferometric studies. Vibrations probably affected the final design of the experimental apparatus more than any other consideration. The original though was to have the entire apparatus as a single unit and portable except for the lack of a handle. However, this idea was abandoned because vibrations from within the apparatus itself disrupted the liquid surface. This led to the separation of the flat and liquid surfaces from the rotating structure resulting in a final setup as pictured in Figure 10. A tabulation of the various components of the experimental equipment as depicted in Figure 10 follows in Table 1.

In the continuing discussion, parenthetic symbols following certain items will help the reader locate them in Figure 10, e.g., (10u) indicates the oscilloscope in Figure 10. Note that some items tabulated are also found in Figure 4.

A cross-like structure (10h) of 3/4-inch aluminum was used to support the laser (10b), rotation gear (10r)

TABLE I

TABULATION OF COMPONENTS OF EXPERIMENTAL EQUIPMENT AS DEPICTED IN FIGURE 10

Symbol	Item
a	Filter for laser power supply
b	Laser
c	Lens
d	Trigger (scope) signal amplifier
e	Adjusting screw for orienting flat
f	Optical flat-wedge
g	Liquid container
h	Supporting cross
i	Front surface mirror (M_3 of Figure 4)
j	Front surface mirror (M_2 of Figure 4)
k	Camera
l	Detector for triggering signal
m	Front surface mirror (M_1 of Figure 4)
n	Detector for level signal
o	Trigger lamp power supply
p	Bridge for support
q	Adjusting screw for orienting cross
r	Rotation gear
s	Drive motor idler
t	Shim plate
u	Scope
v	Drive rim

and detector (10n). Three feet with adjusting screws (10q) were beneath the cross; they were 120 degrees apart and equidistant from the center of rotation of the rotation gear. These feet were used to adjust the beam leaving the rotation gear to be perpendicular to the liquid surface (within 10g). The laser was set on one arm of the cross on kinematic mounts, so that when returned from use elsewhere in the laboratory it could

be positioned exactly as before to maintain alignment. The rubber feet on the laser were replaced with the mounts. The parts of the mount attached to the cross were positioned so that the laser beam passed across the center of rotation. The alignment was done by eye, sighting along the beam and a line drawn on the cross intersecting the center of rotation.

The laser was a Spectra Physics model 130 with 0.3 milliwatt output. The output had a wavelength of 6328 angstroms and a divergence of less than 0.7 milliradian. The laser had dc excitation, but the filtering components, encased in epoxy, were inadequate to eliminate the rectified 60 cycle ripple. An external L-C filter (10a) was built to further decrease this ripple. It was found that this filter decreased the magnitude of the 60 cycle ripple present on the beam by a factor of approximately 10.

A simple mount attached to the cross was used to position the lens (10c) in front of the laser. The lens was one of a set of optician's lenses, all of which had the power measured in diopters. A diopter is 1/f where f is the focal length in meters. The f value needed was approximately 50 cm; therefore, D was approximately equal to 2.0. This particular power was available.

All the mirrors were front surface totally reflective type. The two rotating mirrors M_2 (10j) and M_3 (10i) of Figure 4 were Edmund Scientific Stock Number 30286 aluminized with a protective overcoating. M_1 (10m) was made in this laboratory using Edmund Scientific war surplus flat glass. Gold rather than aluminum was used as the coating material, not so much because of its higher reflectivity at 6328 angstroms but because of the gold crucible set up in the vacuum system at the time of coating. Cleaning consisted of an acetone bath, an Alconox soap bath, a distilled water rinse, a dry nitrogen drying and a 100 degree C oven bake. Deposition was at $.5 \times 10^{-5}$ torr.

Mirror M_1 (note Figure 4) was mounted over an aperture in a flat piece of aluminum. The aluminum and, thus, the mirror were adjustable by three spring loaded 6-32 screws separated by 90 degrees. The spring loading was provided by pieces of neoprene rubber. The mirror was attached so that it just adequately intercepted the laser beam and reflected it downward, thus leaving the reaminder of the aperture clear for the returning reflections to strike the detector by bypassing the mirror M_1 as discussed in the Literature Survey. M_1 and the detector were supported above the rotation gear by a

bridge (10p). M_1 was held at 45 degrees by two 1/4-inch aluminum bars cut at 45 degrees and attached to the bridge. A threaded rod screwed into the bridge supported a threaded aluminum strip to which the detector was attached. A lock nut was used for locking the detector in place, otherwise it could be swung aside for alignment purposes (refer to Figure 10).

The detector employed was an International Rectifier silicon solar cell number SO 510E9 with a peak spectral response at about 0.8 micron. The response was down to about 80 percent at 6328 angstroms. (Other specific curves are illustrated on the Engineering Data sheets[7].) The detector was used as a photovoltaic cell.

The rotation gear (10r) consisted of a bearing, outer race housing and drive rim (10v), drive motor, shim plate (10t) and mirrors, M_2 and M_3. The mirrors M_2 and M_3 were attached to solid triangular shaped blocks with holes cut in the block supporting M_3 so that the laser beam was not obstructed as it passed through the block, struck M_3 and was reflected downward to the flat. Mirror M_3 and its support block are readily discernible in Figure 10. These two support blocks were adjustable by three neoprene spring loaded 4-40 screws separated by 90 degrees (4-40 screws were used because

of their finer adjustment capabilities).

Mirrors M_2 and M_3 and support blocks were mounted via the adjusting screws to a 1/8-inch aluminum shim plate (10t) which was attached to the outer bearing race housing and drive rim (10r). All of this mechanism was rotated with a drive motor. The drive motor was a rubber shock mounted phonograph motor with idler (10s). The idler contacted and rotated the drive rim at about 60 rpm.

The bearing was a deep groove Conrad type taken from a war surplus aerial camera. Since there was little weight involved and thus a small thrust force, this bearing provided adequate support as well as a rotation foundation. The inner race of the bearing was attached to the cross and centered over a hole in the cross. The size of the hole was such that it would not obstruct the sweeping laser beam.

The wedge (10f) was created in this laboratory. It consisted of an Unertl Optical Co. optical flat, a liquid fill and a piece of Edmund Scientific Co. glass plate. The optical flat was 6-inch diameter, 3/4-inch thick crown glass with both surfaces flat to one wave mercury green light and parallel by less than 30 sec of arc. A 5-inch diameter piece of flat glass was cut from

a 3mm thick rectangular piece of Edmund Scientific Co. Stock #60425. This was centered over the optical flat and one edge shimmed up with a 1/8-inch thick shim. This provided a wedge between the upper surface of the flat glass and the lower surface of the optical flat of 0.025 radian. The shim was 1/8 x 1/4 x 3/16 inch with a tapped fill hole in the 1/8 x 1/4 inch side. The flat glass was secured in place over the optical flat with an adhesive sealant, Dow Corning Corp. Silastic RTV 732, applied around the periphery. The result was a liquid container with the sides being the flat glass and optical flat. Squibb mineral oil was used as the liquid fill to provide an optical continuum. There was little if any reflection at the glass-oil interface, since the index of refraction of the three elements was nearly equal, about 1.55 at the sodium D lines. That the reflection was low is evident from the following formula:

$$R = \frac{(n_0 - n_s)^2}{(n_0 + n_s)^2} \qquad (11)$$

where R is the reflectivity at the interface, n_s is index of refraction of the substrate and n_0 is index of refraction of the incident medium. With the human eye, no reflection was visible from one interface, and only an intermittent sparkle from the other. According to

Strong[13], the quantum efficiency of the human eye is about 10 percent at 5100 angstroms, comparable with the best detectors. The 12 percent efficient silicon diode registered this interface reflection, but the interference resulting from this reflection was negligibly small.

The optical wedge was secured in a metal frame with a cork force fit. The frame was attached to 1/4-inch triangular piece of aluminum with adjusting screws (10e), 35.8 cm apart at each corner. Also attached to this aluminum triangle was the liquid container (10g). It was a 9-inch glass cake dish, sandblasted over the bottom to provide a diffuse surface. Krylon flat black paint was sprayed over the bottom to further limit any reflectivity.

The liquid had to have a high viscosity to resist wave motion on its surface, as a result of vibrations. It also had to have an index of refraction near that of the optical flat to provide the proper reflection, R_f approximately equal to R_1. Squibb mineral oil was again found satisfactory for this purpose (its limitations will be discussed in the Discussion of Results).

The optical wedge assembly was placed on a separate table from the one supporting the cross and rotation gear as shown in Figure 10. This placement was

necessary because the rotating structure vibrated the table upon which it sat and consequently caused disturbances in the surface of the mineral oil. The adjusting screws (10e) located 120 degrees and 35.8 cm apart, were used to tilt the complete assembly. Of course, the liquid surface within remained stationary with respect to the earth as the assembly titled. Thus, any magnitude and direction of off-level angle could be created instantly with movement of the adjusting screws.

Alignment

The initial alignment was accomplished by positioning the laser as previously described (refer to Figures 4 and 10). M_1 was adjusted so that the beam struck the shim plate in the center of rotation. A front surface mirror was placed upon the shim plate. When alignment was accomplished, the reflected beam retraced its incident path exactly during rotation of the shim plate. Shims were placed between the shim plate and the outer race housing and drive rim to insure that the shim plate was perpendicular to the incident beam during rotation. M_1 and the shim plate were adjusted concurrently while insuring that the laser beam remained centered on the center of rotation until the reflected beam retraced its

incident path. M_2 was then fixed in position. A right angle prism with hypotenuse and side aluminized was placed aluminized side down and clear side toward M_2 at the position of M_3. M_2 was adjusted until the incident and reflected beams between M_2 and the prism were in a plane above and parallel to the plane of the shim plate. Thus, M_2 was aligned and M_3 was then fixed in position. A mirror was placed over the hole in the shim plate below M_3 to reflect the beam back to M_3. M_3 was then adjusted until the reflected beam retraced its incident path. Liquid was then placed below and the feet on the cross were adjusted so that the reflected beam retraced its incident path. The optical wedge and mineral oil container assembly was then put in place. Thus, alignment was secured.

Data

The data consist of polaroid pictures of oscillographs. Interpretation of this data is easy with the use of Figure 5. Each cycle in the pictures corresponds to the laser beam crossing a fringe. The number of peaks or fractions thereof were counted and with the aid of Figure 5, the angular separation in seconds of the optical flat from level was determined. It must be

remembered that as the beam scanned its circle, it scanned parallel with the fringes twice each revolution. This accounted for the points of minimum frequency or nulls and the points of maximum frequency.

The nulls indicated the direction of the fringes and, thus, the direction of off-level angle. To be meaningful, the oscilloscope sweep had to begin at the same spatial point or time in the beam scan. The direction of the off-level angle could be reckoned with respect to this point. To accomplish this, a Chicago Miniature lamp number 112 in series with a one ohm resistor and powered with a 1.5 volt dry cell (10o) was mounted beneath the rim of the outer race housing and drive rim. Once each revolution its light shone through a small hole in the drive rim and illuminated an International Rectifier silicon solar cell (101) of the SO 510E series mounted on the underside of the mirror M_1 supporting bridge. The output of this silicon chip was fed to a McGohm model 102 P.A. amplifier (10d) which had previously had a voltage divider network added to provide bias, thus, cell operation as a photoelectric cell or photodiode, though this was probably not necessary with the present signal. The output of this amplifier was sufficient to trigger the oscilloscope which

required an exceedingly high trigger level. The oscilloscope (10u) was a dual-beam Tektronics type 502A with a Polaroid camera mount, Tektronics C-19, and camera (10k). It had a frequency response down to dc which readily allowed recording of the data, all of which were below 100 cps.

All data were viewed two or three times to insure duplication. Typical data are shown in Figures 11 and 12. Each subfigure, unless otherwise noted, has one set of numbers followed by another set. First is the off-level angle interpreted from Figure 5, followed by the direction of the off-level angle or intersection of the planes of the oil and flat, referenced to the beginning of the scope sweep as zero degrees. Of course this later figure could be $\pm$ 180 degrees. A discussion on this will follow in the Discussion of Results.

The oscilloscope horizontal sweep rate was 0.2 sec/cm for all the pictures unless otherwise noted. The vertical sensitivity was 0.1 mv/cm for most of the pictures, though it was 0.2 mv/cm for some. The laser's continued loss of power while the data were being taken caused the shift to 0.1 mv/cm sensitivity to maintain a similar vertical deflection. The output of the laser

just before completion was down to 0.02 milliwatt from the rated 0.3mw.

This oscilloscopic horizontal sweep rate permitted about 1.8 laser beam revolutions and concomitant interference phenomena to be registered on the oscillographs. This means there are 13.1 degrees of revolution corresponding to each small division on the horizontal scale. Assuming the nulls can be read to a half division, the direction of the off-level angle can thus be read to about $\pm$7 degrees. Fringe count will be to 1/2 fringe corresponding to off-level angle accuracy of less than $\pm$0.2 sec, magnitude-wise.

Figure 11a shows the signal from the optical flat only as received from the manufacturer. From the figure, it is determined that there are between seven and eight fringes per revolution, say 7-1/2; thus, the sides are non-parallel by 2.5 sec. Figure 11b shows the signal from the optical flat after it was transformed into an optical wedge as described previously. This signal was the result at the detector of the reflection from the lower surface of the optical flat and the reflection from the oil-glass interface at the top of the flat. The fact that this signal exists shows that the indices of refraction of the optical flat and oil were not

exactly equal. Again this signal indicates that the optical flat was itself a wedge of 2.5 sec. It should be noted that the signal from the rectified 60 cycle of the laser power supply superimposed upon the laser beam as mentioned in the Literature Survey was of about the same amplitude as the before-mentioned signal. The level of both was about 0.05mv, well below the signal that was to indicate the level as can be verified in Figure 11c. Figure 11c is expanded on the horizontal scale with a sweep rate of 0.1 sec/cm to show detail and allow a count. The following subfigures of Figures 11 and 12, except 12e and 12f, are self-explanatory with the aid of previous comments.

It should be noticed how the vertical deflection increased with decreasing off-level angles. This was caused by the loading effect on the detector. As the reflected beams, R_f and R_1 of Figure 1, overlapped to a greater extent because of a smaller off-level angle, the interference phenomena on the detector caused a larger ac signal.

The magnitude and direction of the off-level angles can be readily determined down to about 2.5 sec of arc. With smaller angles, difficulties arise as are evidenced in Figures 12e and 12f. Further information on these

difficulties will appear in the Discussion of Results. The off-level angle can be determined still by the number of fringes per revolution. However, the direction cannot be determined consistently. The nulls are evident in Figure 12f however, and thus the direction of the angle can be determined. Figure 12f concludes the data. The specimens shown are quite representative and are only a sampling of the various angles and directions created and displayed on the oscilloscope.

DISCUSSION OF RESULTS

The results were as expected. No electrical noise as such was visible in the signal. Of course, noise might have been evident if the 60 cycle ripple had been completely removed. In any event, the noise level would not have obscured the signal. From the data, it can be determined that a 10 percent intensity variation at the steepest part of the curves could be discerned above the noise-level. This would make the value of the maximum sensitivity for out of level detection of 1.06×10^{-2} sec, calculated in the Literature Survey, valid.

The difficulties evident in Figures 12e and 12f can be attributed to the instability of the building. The laboratory floor was continuously shifting and tilting by a few seconds of arc. This was verified visually. The whole of the flat was illuminated with an expanded collimated laser beam and fringes formed over the whole wedge area. These were viewed by capturing the reflected beam with a large diameter lens and placing the eye at the focal point. The flat was adjusted to be as parallel to the liquid surface as possible. The fringes were seen to "squirm" continuously. They increased in number, decreased and changed

orientation. The movement of a person about the laboratory caused an increased "squirming". The periods of the shifting were smaller than the period of the scan. Thus, an adjusted angle, for example, two seconds, would be increased, decreased and/or changed in orientation during a scan as the laboratory floor tilted. Of course the smaller the adjusted angle, the greater the effect of the tilting laboratory floor. For example, 1 second adjusted angle would change orientation by 45 degrees if the laboratory floor tilted 1 second in a direction 90 degrees from the direction of the adjusted angle. With greater adjusted angles, the floor tilt had less effect.

The above was an unsuspected realization from the study. Objects or structures cannot be leveled to the ultimate capabilities of this device unless they behave levelly. Needless to say, the above encountered difficulty prevented any ultimate accuracy determination, but an extrapolation can be made.

However, at this point something must be said about the quality of the optical flat. It is flat to less than one wavelength mercury green (manufacturer's specifications). This is the 5461 angstrom line, equal to 5.46×10^{-5} cm. The "non-flatness" of this optical

flat would cause a variation in signal intensity of almost three complete fringes. Obviously the optical flat was flat to far less than 5.46×10^{-5} cm. Or, at least, it was "flatter" in the area of the scan circumference. It should be noted that the non-parallelism of the sides of the optical flat were also far less than the guaranteed 30 seconds. At any rate the irregularities of the optical flat would prevent any angular determinations of the order of 10^{-2} seconds of arc as suggested in the Literature Survey. It would also make angular determinations less accurate than indicated by the data. The principles involved make this fact immaterial in a feasibility study.

Optical flats 5 inches in diameter can be readily obtained commercially, flat to 10^{-6} inch. Optical flats "flatter" than this are a rarity, but can be obtained. The 10^{-6} inch would cause a change in intensity at the steepest part of the curve in Figure 2 of about 25 percent of the maximum intensity. Double this "noise" value, 50 percent change in intensity would be the minimum discernible. This corresponds to a minimum detectable angle of about 0.1 second.

The question arises, can the flat be mapped? Theoretically, yes, but practically, no. The support

structure is too unstable, heat currents cause the table to tilt and the whole building sways. A person walking down a corridor outside the laboratory will tilt the laboratory floor by as much as 10 seconds, and walking from the corridor to a position beside the experimental setup will tilt the laboratory floor by as much as 25 seconds. However, a recent investigation[12] indicates that this mapping can be done. A somewhat different setup but similar principles were used with good results. The results indicate that the ultimate sensitivity as theorized in this study is obtainable.

Of course, an optical flat could be mapped for irregularities and these irregularities compensated electronically so that only the signal resulting from angular separation of wedge surfaces remained. In any event there are possibilities for obtaining an optical flat that is effectively a plane, thus not limiting the sensitivity of the device in any manner.

As the off-level angle decreases, the interference phenomena indicate that a closer and closer examination of the wedge surfaces is made. But at angles larger than about 3 seconds, the interference of the wedge predominates over that caused by irregularities in the wedge surfaces and criterion for measuring set forth

earlier remains valid. The observed upper limit of detectable angle approached 40 seconds. This was less than the 74 seconds maximum detectable angle calculated in the Literature Survey. The probable reason for the 40 second limit was the consideration of inadequate beam overlap. The 74 seconds were obtained by assuming 1/2 beam diameter overlap. Referring to Figure 8 and the equation for maximum detectable angle, $\theta=((a/2)-0.037)/2d$, it can be seen that θ equal to 40 seconds required approximately a 60 percent beam diameter overlap. The 60 percent overlap yielded the minimum detectable interference phenomena corresponding to the maximum 40 second angle. This was not unreasonable, considering the irregularities in the interfering wave fronts caused by the multiple reflections from imperfect surfaces.

The direction of the angle cannot be determined with great accuracy however. At best the accuracy is $\pm$ 7 degrees, and it has a 50 percent probability of being $\pm$ 180 degrees also. The 180 degree uncertainty can be eliminated quickly. The wedge angle can be varied in the assumed direction. More fringes will appear if the angle increases and, depending on whether the edge of the flat was raised or lowered, will determine the

direction. However, this accuracy in determining the direction is as accurate as any existing device to the author's knowledge. If any object is being leveled, it can be caused to approach the level so closely as to make the direction of the off-level angle meaningless. Prompted by the data contained herein and the results of Roesler[12], the author believes that angles of the order of 10^{-2} seconds of arc can be determined.

From the Literature Survey, the effects of variables such as the diameter of the optical flat and scan and the wavelength of illuminating radiation are obvious. Other changes in the system that would affect the appearance of the data would be to make the wedge surfaces highly reflective creating multiple beam interference. For instance, one could aluminize the flat and use mercury for the liquid. Vibration surface waves in the mercury could be controlled with an overlay of oil which could also be used as the wedge composition. The result would be sharper, better defined fringes than are the cosine squared fringes. The particular advantage, if any, of this method is not obvious to the author at this time.

Following is a discussion of a possible means of automating or closing the control loop on the device;

a method to make it self-seeking of the level. Two of the three adjusting screws on the optical wedge assembly discussed in the experimental procedure used to vary the off-level angles for data recording are replaced by a stack of piezo-electric crystals[11]. The other adjusting screw remains as a pivot point. The off-level angle is then controlled by the voltage applied to the piezo-electric crystals. The nulls which indicate direction are detected by means of RC circuits. The time constant is such that the capacitor will not discharge to a set level indicating a null except at the nulls where the pulses are spaced far enough apart time-wise. Of course, the time constant will have to be varied with the number of fringes. A scan is made; both a count and null recognition are made. Of the two stacks of control crystals, the one nearest a null is expanded a set increment to raise the flat on that side. Another scan is made to allow the system to equilibrate. Then another count and null recognition are made. If the count is greater than before, the null location is ignored and the previously expanded crystal is contracted by two increments. If the count is less, again the crystal nearest a null is expanded. This procedure is continued until the count is zero.

When the count is zero, another procedure is used to further level the flat. While a count is continued for each revolution to insure that it remains zero, a sampling of the intensity of the interference phenomena is taken as the scan crosses each crystal stack and pivot. The intensity over the two stacks is compared with that over the pivot and the stacks are adjusted accordingly. Thus, the device will seek the level automatically to the degree of accuracy desired.

The object to be leveled, of course, has an initial known position with respect to the optical flat, the voltages applied to the crystals then represent the amount of feedback required to reposition the object to cause it to be level.

Another possible application of this device, modified somewhat but using the same principles, would involve alignment procedures over laboratory distances. The great coherence length of the laser could make this feasible providing the laboratory atmosphere is not too turbulent. Of course, mirrors or optical flats would provide the reflective surfaces instead of the liquid and optical flat used herein.

CONCLUSIONS

The optical interference level described in this study was found to possess the following capabilities and characteristics:

(1) Sensitivity was determined to be ± 0.01 seconds of arc.

(2) The minimum off-level angle was not obtained (see Discussion of Results). The nulls indicated the direction of the off-level angle to within $\pm$ 7 degrees.

(3) The maximum dynamic range was 40 seconds of arc.

These measurements are absolute (no calibration necessary). These capabilities make this device unexcelled for determining the measure of level, to the author's knowledge. However, the ultimate capabilities of this device were not realized, due to deficiencies in optical components and instability of the floor of the laboratory.

BIBLIOGRAPHY

1. Born, M. and Wolf, E., Principles of Optics, 3rd Rev. Ed., Pergamon Press, London, 256 (1965).

2. Ibid, p. 259.

3. Ibid, p. 619.

4. Burgess, T. J., Effect of High Velocity Mirror Translation on Optical Coherence in Laser Interferometers, (AEC Contract No. w-7405-eng-48), University of California Lawrence Radiation Laboratory, Livermore, California, Oct. 8, 1965.

5. Ditchburn, R. W., Light, 2nd Ed., Interscience Publishers Inc., New York, Vol. 2, 536 (1963).

6. Emerson, W. B., Journal of Research of the National Bureau of Standards, 49; 241 (1952).

7. International Rectifier Corp., Engineering Data Sheets, El Segundo, California.

8. Liberty Mirror, (Private Correspondence), Brackenridge, Pa., March 29, 1966.

9. Martin, L. C., Optical Measuring Instruments, Blackie and Son Limited, London, 270 (1924).

10. Oppenheim, V. and Jaffe, J., American Journal of Physics, 24; 610 (1956).

11. Ramsay, J. and Mugridge, E., Journal of Scientific Instruments, 39; 636 (1962).

12. Roesler, F. L. and Traub, W., Applied Optics, 5; 463 (1966).

13. Strong, J., Concepts of Classical Optics, W. H. Freeman and Co., San Francisco, 488 (1958).

14. Van Der Ziel, A., Solid State Physical Electronics, Prentice-Hall, Inc., Englewood Cliffs, N. J., 291 (1957).

APPENDIX A

The following relationships utilized in the body of this Thesis will be derived from and applicable to Figure 9. The relationship of ϕ_2 to ϕ_1 and the lateral displacement of R_f from R_1 will be determined.

First, the relationship of ϕ_2 to ϕ_1. Utilizing Figure 9 and the laws of refraction at small angles associated with the incident ray I_i,

$$\theta_2 = \theta_1/n_g, \tag{1}$$

where n_g is the index of refraction of the substrate or glass wedge. The index of refraction of the incident medium (air) is assumed equal to 1. Also

$$\theta_3 = \theta_1-\theta_2. \tag{2}$$

With reference to ray R_f and again the laws of refraction at small angles,

$$(\theta_3+\theta_1)n_g = \theta_1+\phi_2. \tag{3}$$

Substituting the value of θ_2 from Equation 1 into Equation 2 and the value of θ_3 from Equation 3 into Equation 4 yields,

$$((\theta_1-\theta_1/n_g)+\theta_1)n_g = \theta_1+\phi_2$$

$$\phi_2 = 2\theta_1(n_g-1). \tag{4}$$

From the fact that ϕ_1 equals θ_1 and the assumption that n_g equals 1.5

$$\phi_2 = \phi_1. \tag{5}$$

Secondly, from Figure 9,

$$d = \theta_4 h. \tag{6}$$

Again from the laws of refraction at small angles,

$$\theta_4 = \theta_3 n_g. \tag{7}$$

Utilizing Equations 1 and 2 and substituting the value of θ_4 for Equation 7 into Equation 6 yields,

$$d = \theta_1 h (n_g - 1). \tag{8}$$

Again, from the fact that ϕ_1 equals θ_1 and the assumption that n_g equals 1.5,

$$d = \phi_1 h (.5). \tag{9}$$

From Equation 9 and Figure 9, it is obvious that the lateral displacement of R_f from R_1 is less than 2d, which of course is less than $\phi_1 h$.

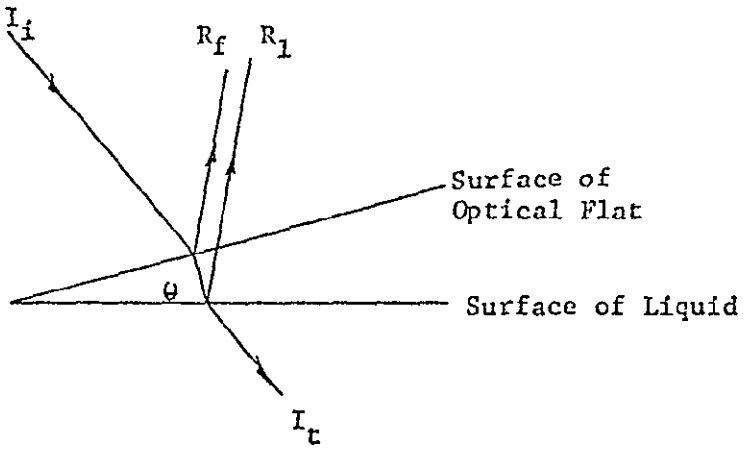

ILLUSTRATION OF ORIGIN OF INTERFERING RAYS R_f AND R_1 IN AN OPTICAL WEDGE

FIGURE 1

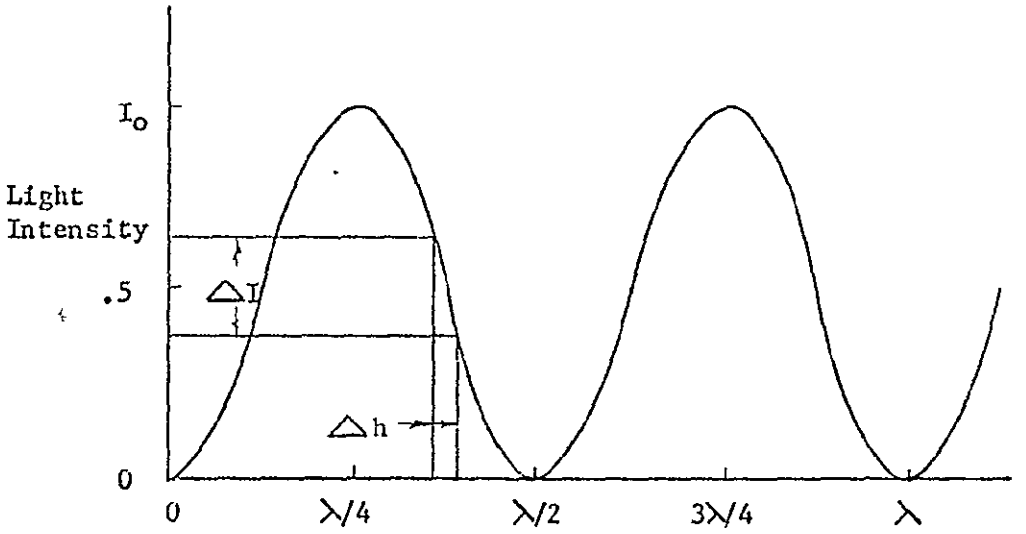

LIGHT INTENSITY VERSUS SURFACE SEPARATION IN AN OPTICAL WEDGE

FIGURE 2

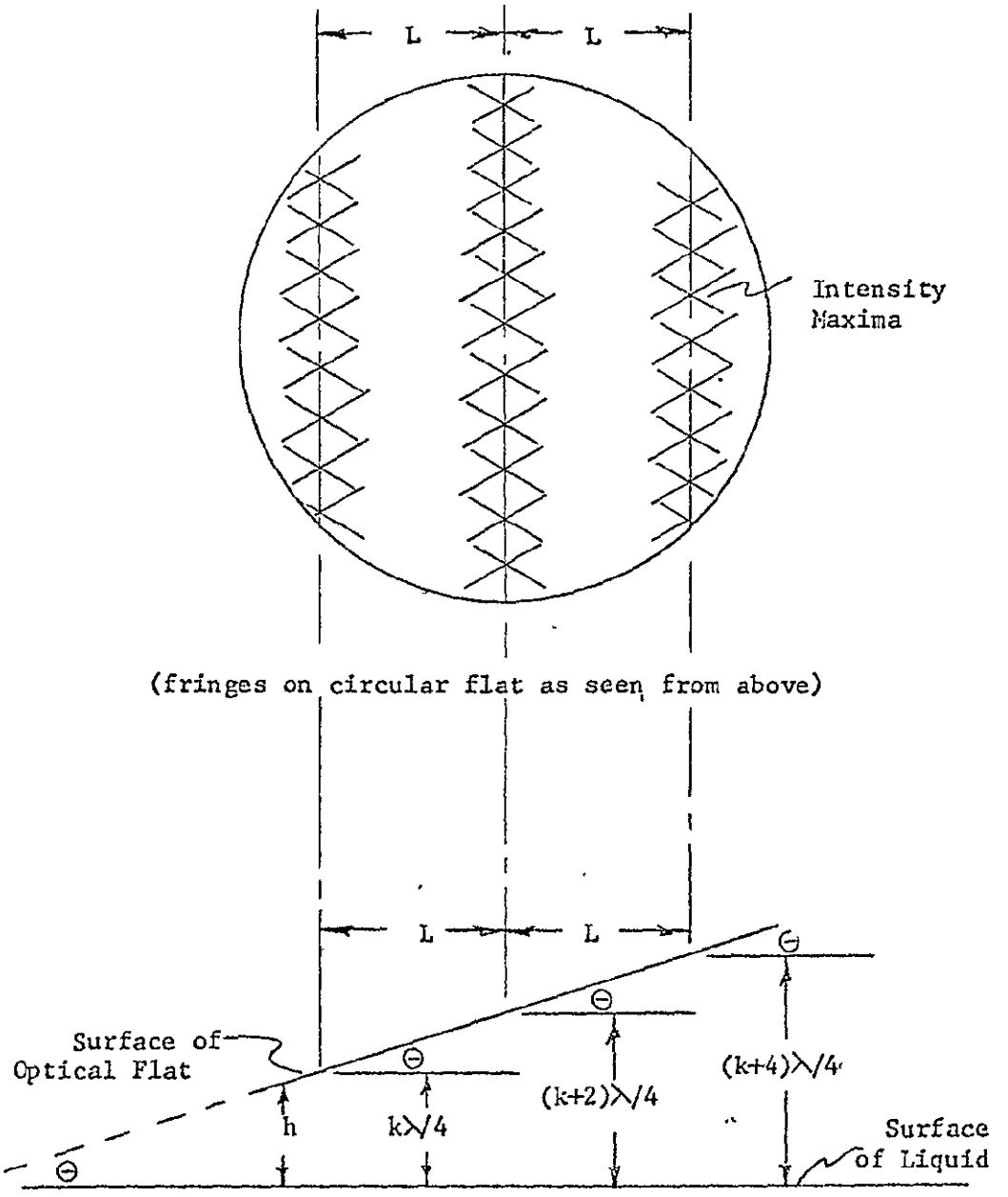

LOCATIONS OF INTERFERENCE MAXIMA WITHIN AN OPTICAL WEDGE

FIGURE 3

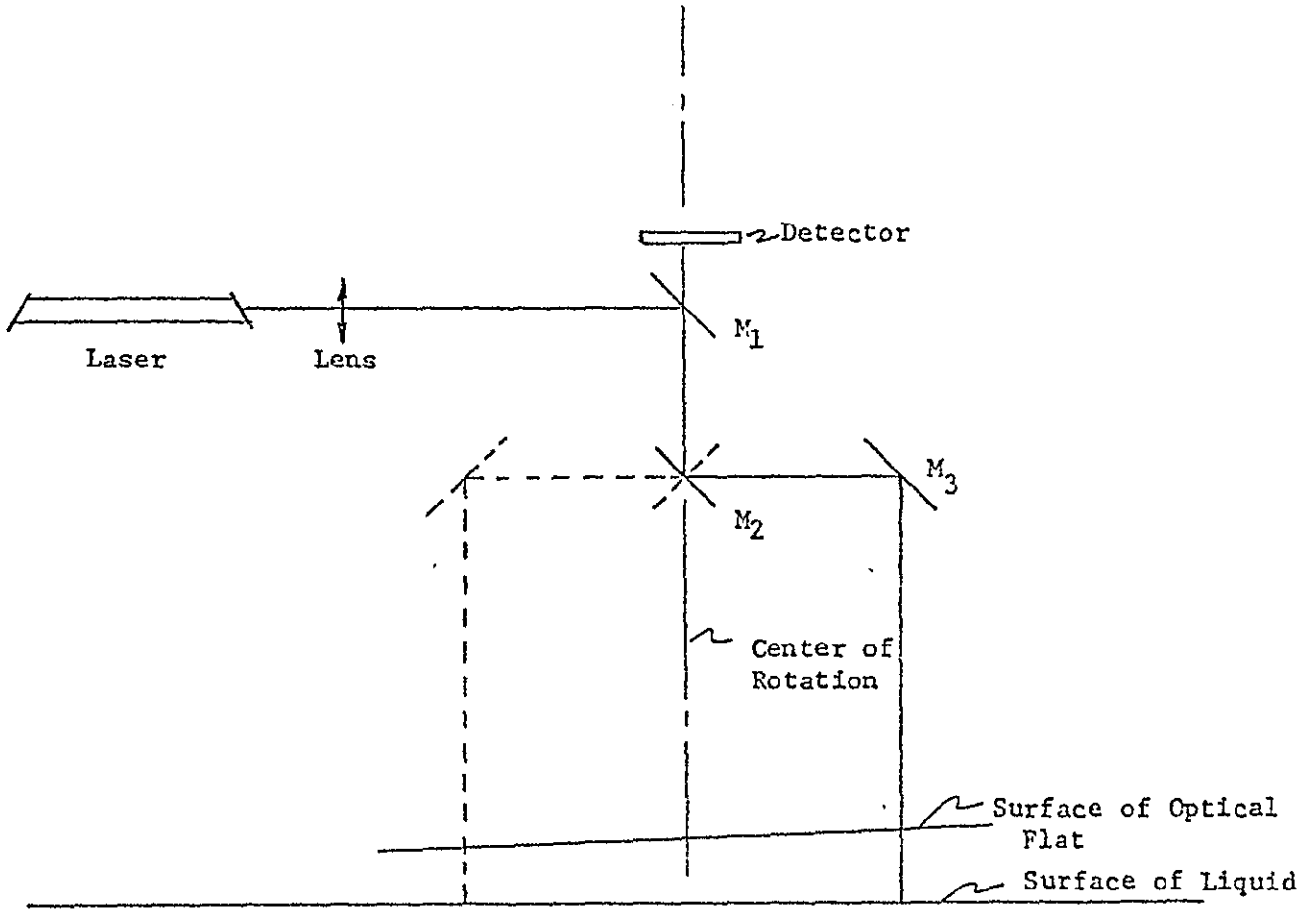

DIAGRAM OF EXPERIMENTAL SETUP

FIGURE 4

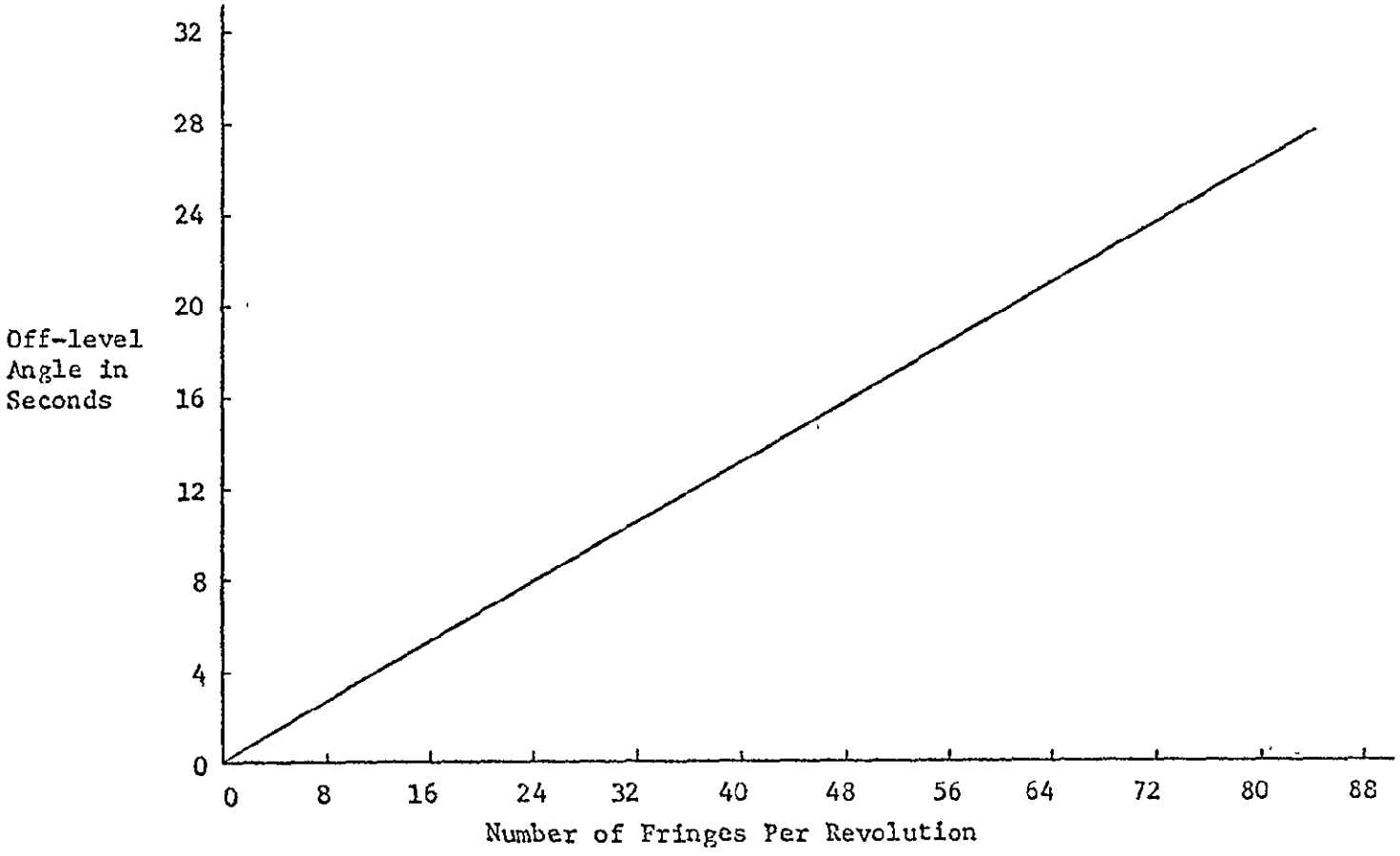

PLOT OF WEDGE ANGLE VERSUS NUMBER OF FRINGES PER REVOLUTION

FIGURE 5

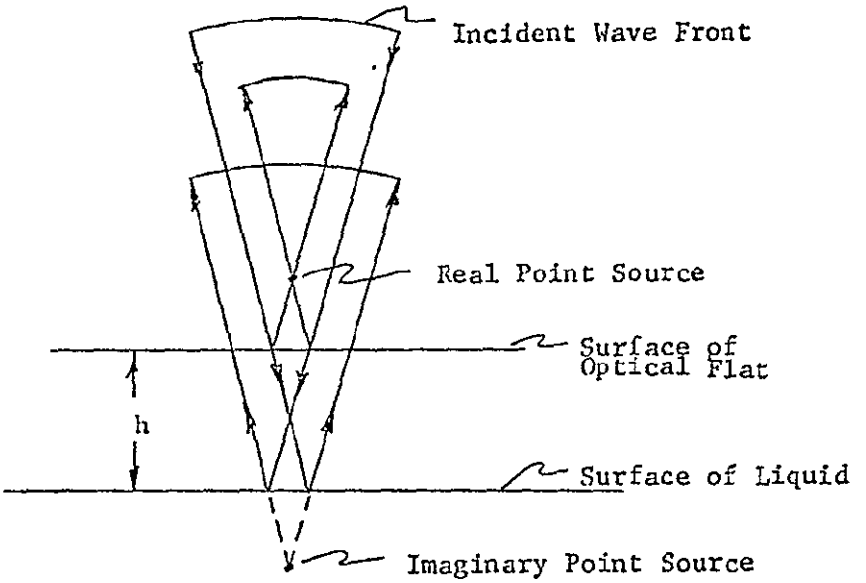

ILLUSTRATION OF FORMATION OF POINT SOURCES SEPARATED IN DEPTH

FIGURE 6

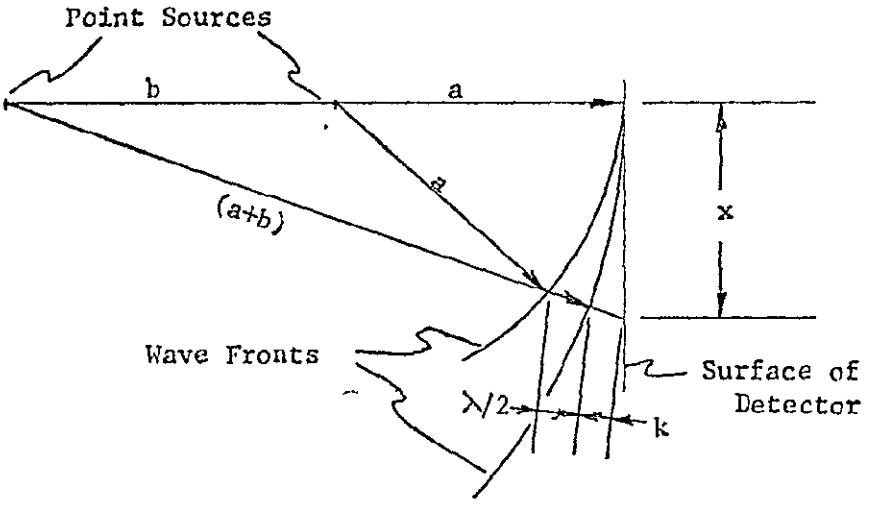

ILLUSTRATION OF THE RADIUS OF THE FIRST FRINGE RESULTING FROM TWO POINT SOURCES SEPARATED IN DEPTH

FIGURE 7

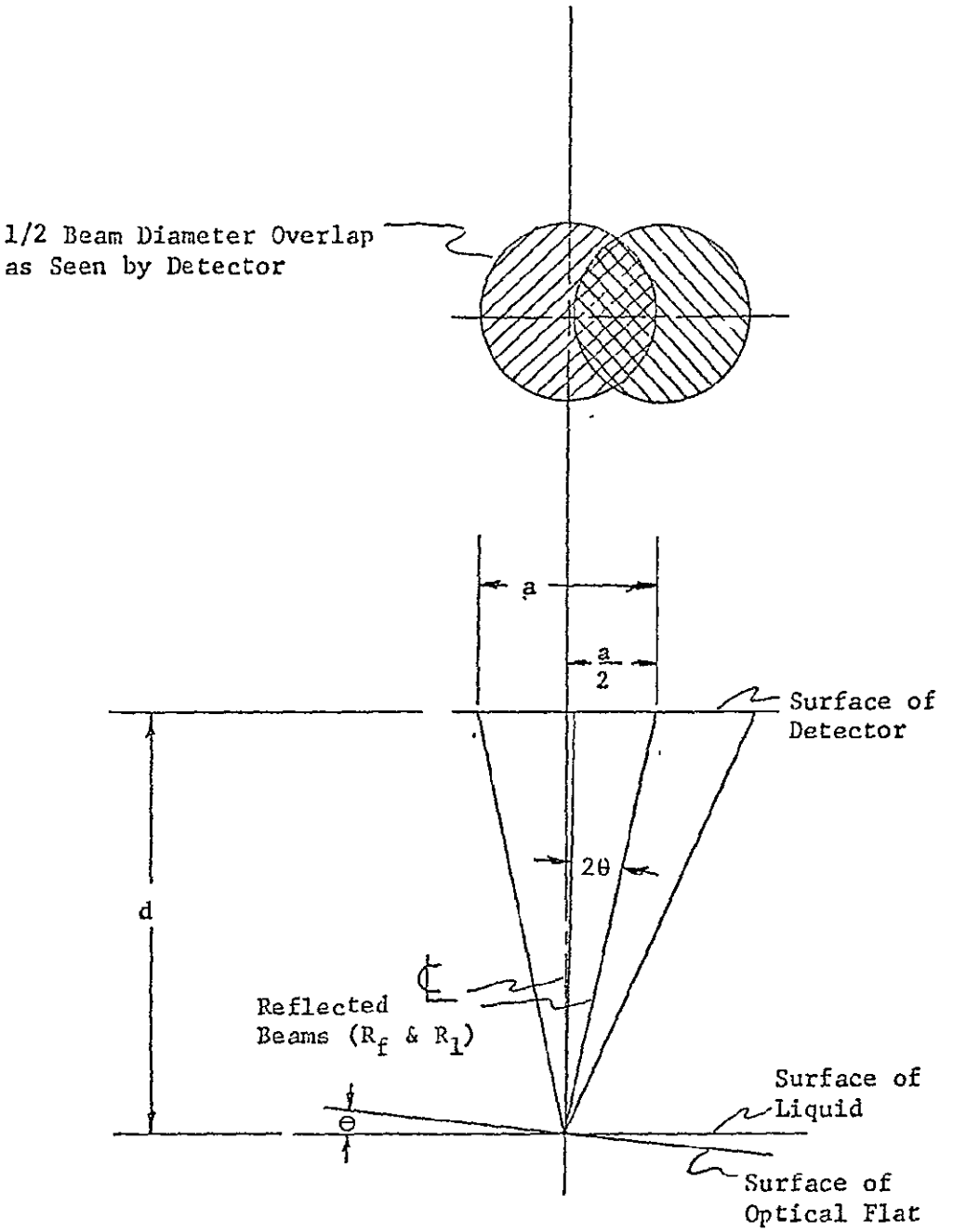

ILLUSTRATION OF OVERLAP OF REFLECTED BEAMS
FROM SURFACES OF LIQUID AND OPTICAL FLAT

FIGURE 8

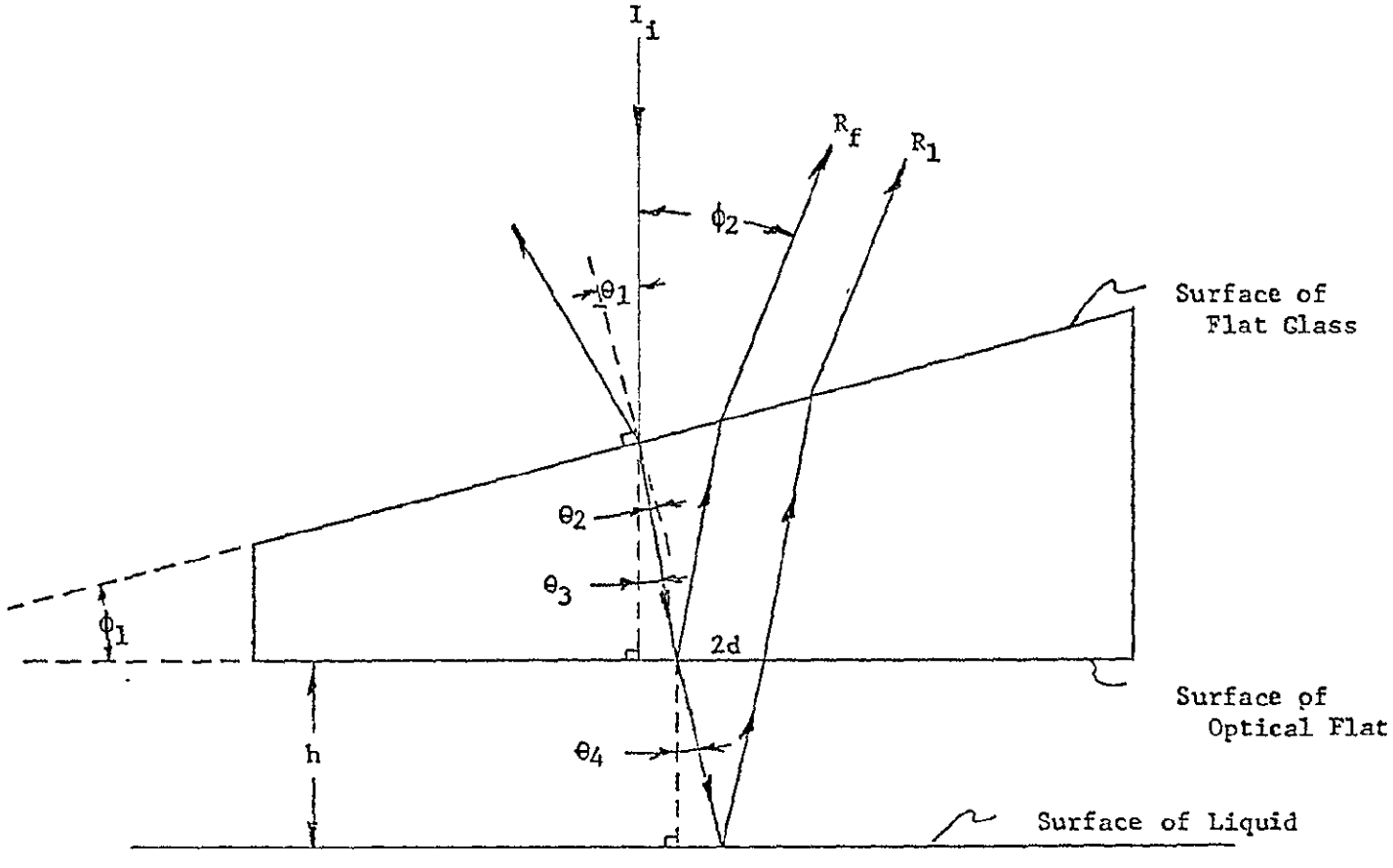

ILLUSTRATION OF ISOLATION OF R_f AND R_1 FROM OTHER REFLECTIONS BY USE OF WEDGE OF ANGLE ϕ_1

FIGURE 9

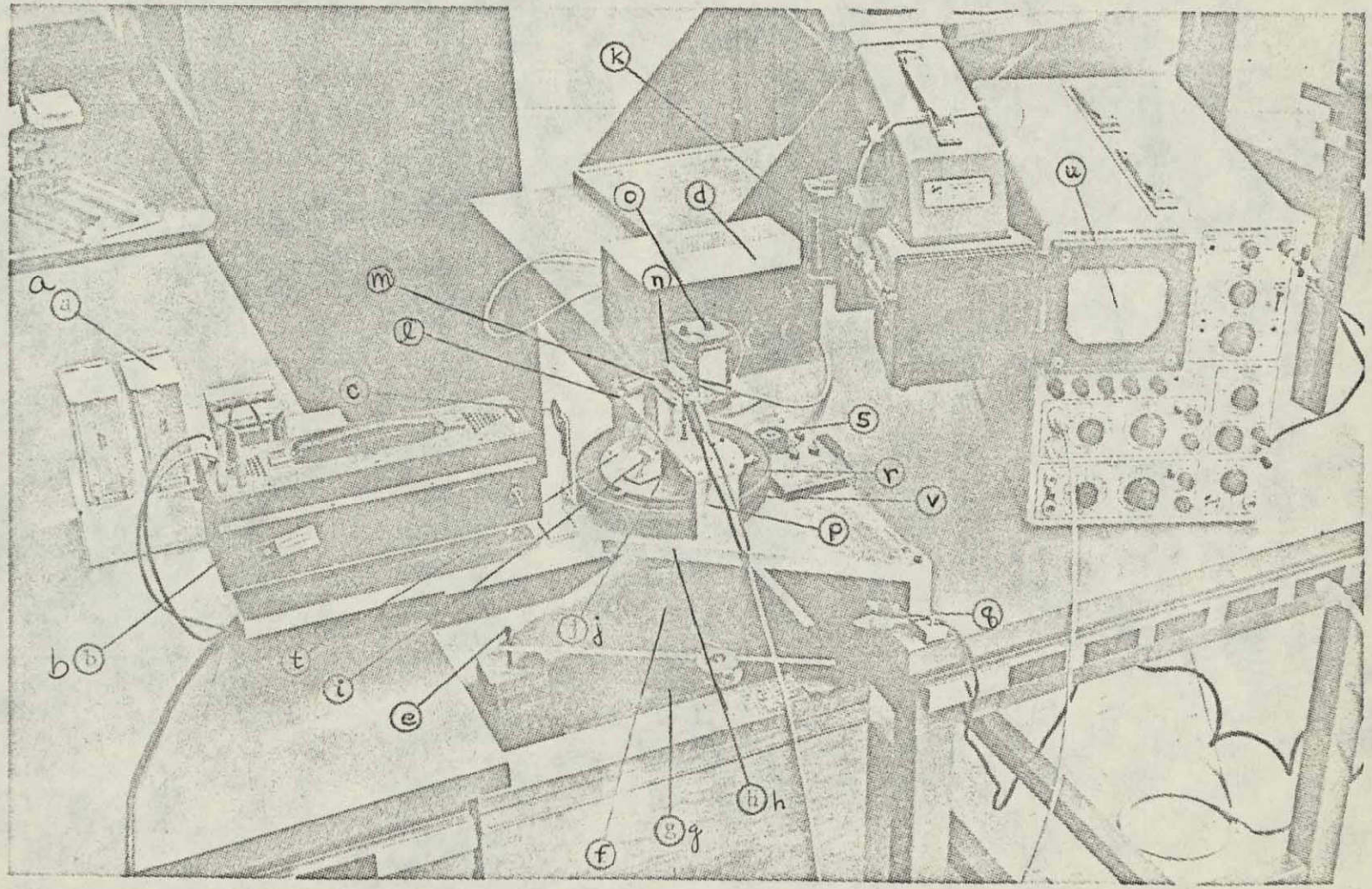

PICTURE OF EXPERIMENTAL SETUP

FIGURE 10

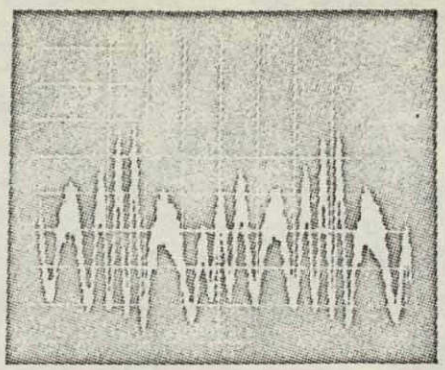

Angle: 2.5 sec

(a)

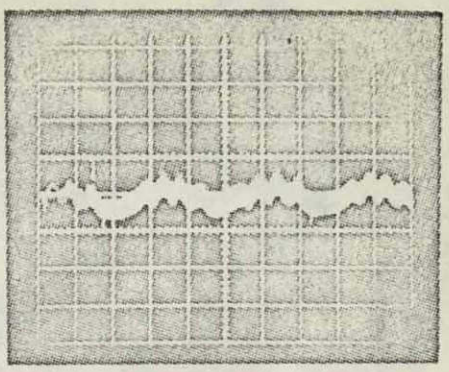

Angle: 2.5 sec

(b)

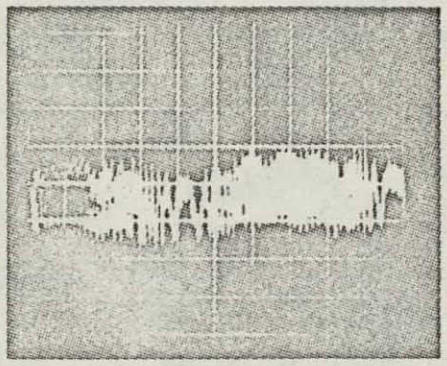

Angle: 30.2 sec
Direction: 135°
(c)

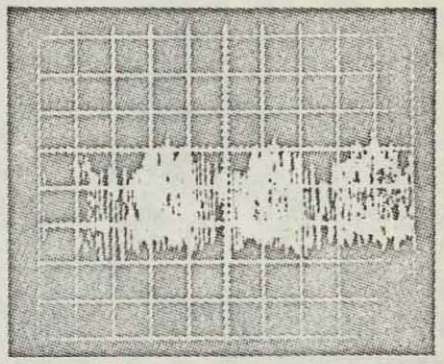

Angle: 21.2 sec
Direction: 145°
(d)

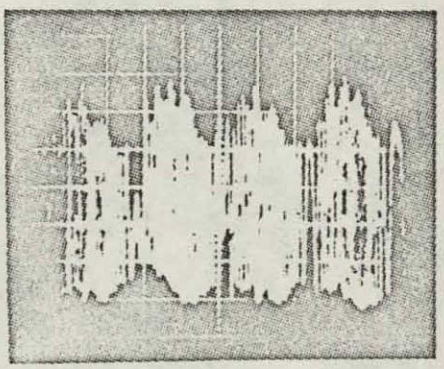

Angle: 15.5 sec
Direction: 30°
(e)

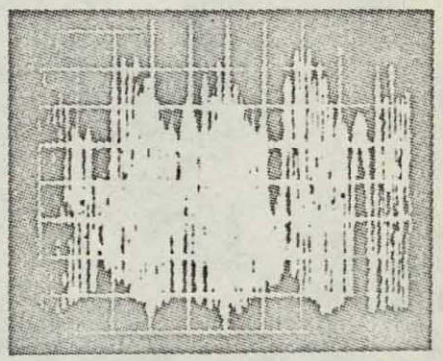

Angle: 7.4 sec
Direction: 128°
(f)

OSCILLOGRAPHIC DEPICTIONS OF OFF-LEVEL ANGLES

FIGURE 11

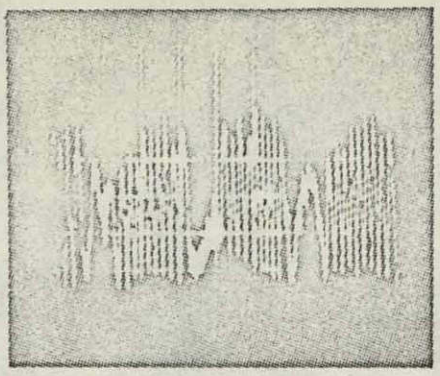

Angle: 6.5 sec
Direction: 130°
(a)

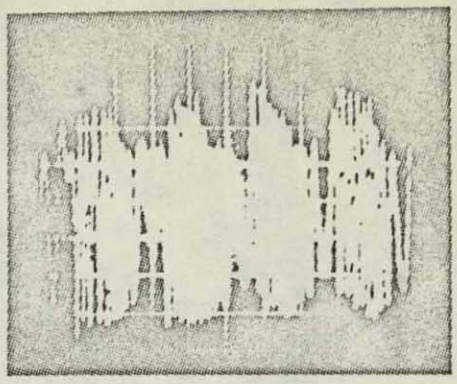

Angle: 6.4 sec
Direction: 40°
(b)

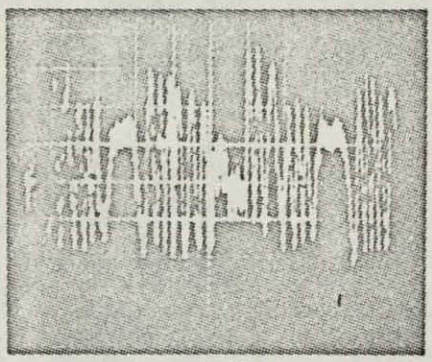

Angle: 4.5 sec
Direction: 175°
(c)

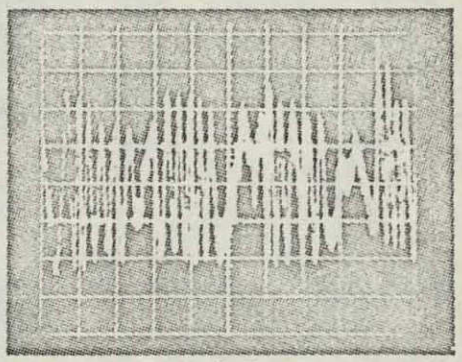

Angle: 4.5 sec
Direction: 165°
(d)

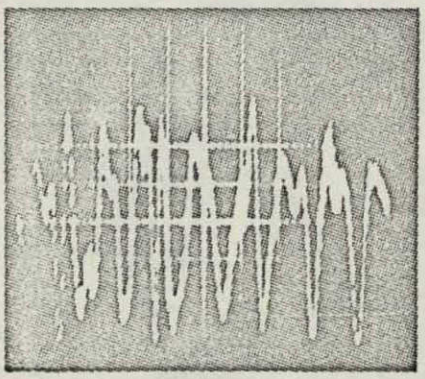

Angle: 1.8 sec
Direction: ---
(e)

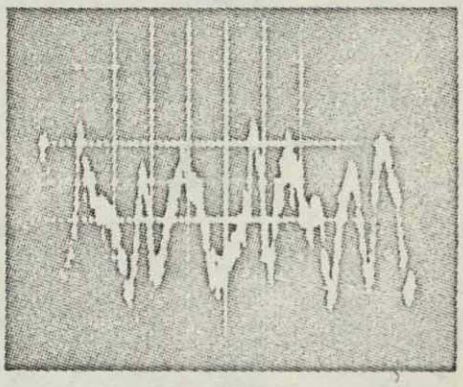

Angle: 1.3 sec
Direction: 120°
(f)

OSCILLOGRAPHIC DEPICTIONS OF OFF-LEVEL ANGLES

FIGURE 12